國立臺灣大學理學院天文物理研究所

碩士論文

Graduate Institute of Astrophysics

College of Science

National Taiwan University

Master Thesis

以 GOODS-North 的星系檢驗塵埃吸收跟紫外線光譜斜率的關係

The Correlation between Dust Absorption and UV Spectral Slope
of Galaxies from the GOODS-North

李仕卿

Si-Heng Lei

指導教授：王為豪 博士　孫維新 教授

Advisor: Wei-Hao Wang, Ph.D.　Wei-Hsin Sun, Prof.

中華民國 101 年 7 月

July, 2012

誌 謝

　　本論文是在我的導師王為豪博士的悉心指導下完成的。他嚴謹的科學態度，精益求精的工作作風，平易近人的個性深深地感染和激勵著我。從課題的選擇到最終完成，王為豪老師都始終給予我細心的指導，在此謹向王為豪老師致以誠摯的謝意。

　　感謝孫維新老師對我的栽培。他細心指導我的學習，在此，我要向孫維新老師表達由衷的感激。

　　感謝我的家人，感謝媽媽為我所付出的一切。養育之恩，無以回報，她永遠健康快樂是我最大的心願。

　　從開始進入課題到論文的順利完成，有多少可敬的師長、同學、朋友給了我許多的幫助，在這裡請接受我誠摯的謝意。

中文摘要

在我們研究星系的恆星形成率的時候，我們很難測量到無線電波的輻射，加上我們清楚知道年青大質量恆星是如何輻射紫外線，所以我們可以透過觀測星系的紫外線，再推算出紫外線的恆星形成率。此過程必須知道星系中的塵埃吸收了多少紫外線，再把被吸收的量修正回去，從而得到正確的紫外線亮度並推算出恆星形成率。由於在星爆星系中，星系的紫外線光譜斜率(β)和其塵埃吸收有相關性，因此現時天文學家主要相信塵埃吸收和星系的紫外線光譜斜率(β)有關，由 $f_\lambda = \lambda^\beta$ 定義，其中 λ 在 1300-3500 Å 之間。本論文希望再次檢驗上述關係，先由 Morrison et al. (2010)得到星系的無線電波亮度，由星系的無線電波亮度得到無線電波恆星形成率。星系無線電波的產生主要因為大質量年老恆星在超新星爆炸的時候，相對論性的電子被磁場加速，進而產生無線電波的同步輻射，加上無線電波不受塵埃吸收的影響，因此可以由無線電波恆星形成率和紫外線恆星形成率的比值推斷塵埃吸收的本質，再檢驗這和 β 是否相關。

在星系紫外線的亮度和紅移方面，本次工作採用了 Barger et al. (2008)的 GOODS-N 星系目錄，其紅移範圍比以往的分析廣，該目錄中同時有 1.4 GHz 的天體最高紅移到達 z~2.6。在星系無線電波的亮度方面用了 Morrison et al. (2010)的 VLA 1.4 GHz GOODS-N 星系目錄，再運用 Wang et al. (2012)的方法把到無線電波的亮度推導出無線電波的恆星形成率，此為不受塵埃吸收影響的恆星形成率。在比對無線電波恆星形成率和紫外線恆星形成率的比值和 β 後，我們並沒有發現它們之間有很強的相關性。我們再引入星系的 z - Ks 顏色，並以 $z - K_s$ vs. β 的關係定義出兩個新參數，嘗試找出此參數與 β 的關係，但我們仍然沒有看到參數與 β 之間有很強的相關性，因此判斷 β 和塵埃吸收之間並沒有很強的相關性。

關鍵字：恆星形成率，紫外線光譜斜率，星系，塵埃吸收，GOODS North

ABSTRACT

When we study star formation rate (SFR) of high redshift galaxies, because we know well how young high mass stars emit UV radiation, we observe the rest-frame UV emission of galaxies, and convert it to UV star formation rate (UV SFR). We also need to know the dust absorption in the UV, and then correct for the absorbed part to obtain the intrinsic UV luminosity and SFR. It is widely believed now that dust absorption is correlated with the rest-frame UV spectral slope (β) of a galaxy, defined as $f_\lambda = \lambda^\beta$, where λ is between 1300-3500 Å in this work. This work aims to verify the above correlation; we will derive the radio SFR from the radio flux of galaxies from the radio catalog of Morrison et al. (2010). The radio emission is generated by supernova explosion from high mass stars, in which relativistic electrons are accelerated by magnetic field and produce synchrotron radiation. Therefore the radio emission can also infer high mass star formation rate. Since the radio emission is not affected by extinction, the radio-to-UV SFR ratio can indicate dust absorption. Thus we can test if there are any correlations between the UV and radio SFR ratios and β.

For the rest-frame UV fluxes and redshifts, this work uses the GOODS-N catalog from Barger et al. (2008). This catalog covers a broader range of redshift, compared to other works, and the highest redshift object in this catalog with 1.4 GHz radio flux is about z~2.6. We adopt the VLA 1.4 GHz GOODS-N catalog from Morrison et al. (2010) and use the method in Wang et al. (2012) to convert the radio flux to radio SFR. After comparing β with radio-to-UV SFR ratios, we find that there is no strong correlation between them. Then we include $z - K_s$ colors of galaxies and use a $z - K_s$ vs. β diagram to define two new parameters to test if they are correlated with extinction. We do not

find significant correlations. Therefore, we conclude that there is not a strong correlation between dust absorption and β.

CONTENTS

LIST OF FIGURES

LIST OF TABLES

Chapter 1   Introduction

To understand the evolution history of galaxies, we need to know their star formation rate (SFR). There are several methods to estimate SFR of a galaxy, such as UV SFR, radio SFR, Hα SFR, and Far-IR SFR. In particular we know well enough about stars. Young high mass stars emit strong UV radiation, so we can convert the UV flux to UV star formation rate (UV SFR). Because it is easier to observe in the optical, the UV SFR is commonly used to infer the evolution history of galaxies. On the other hand, UV radiation is largely affected by dust absorption. If we do not correct for the absorbed radiation, the UV SFR would be underestimated.

Many works (Meurer et al. 1999, Bouwens et al. 2011) try to use the UV spectral slope (β, as defined in Chapter 3) to correct for the absorption in the UV. People believe that β is correlated with extinction, so we can convert β to extinction to correct for the absorption in the UV. In this work, we verify whether β correlates with extinction.

We also include a longer wavelength color, $z - K_s$. By comparing the long wavelength color and short wavelength color (β), we construct a $z - K_s$ vs. β diagram described in Chapter 5. We define a new parameter in the new diagram to find if there is correlation with β based on the assumption that the direction of extinction follows a trend in the $z - K_s$ vs. β diagram. We also define β_a to find if there is correlation with β based on the assumption that the evolution of stellar population follows the trend. All the tests show that β is not a good extinction indicator.

Chapter 2   Data

In this work, we need rest-frame UV to infer UV star formation rate. It's well known that UV radiation is produced by OB stars in a galaxy, so we can obtain star formation rate of OB stars in a galaxy via calculate the UV flux of it.

We adopt the catalog of Barger et al. (2008) which have 2626 objects with redshift, which KPNO U band magnitudes are from Capak et al. (2004), and the F435W, F606W, F775W, and F850LP magnitudes are from the HST Advanced Camera for Surveys (ACS) observations of the GOODS-N (Giavalisco et al. 2004). The limiting magnitudes, central wavelength and full width half maximum (FWHM) are listed in Table 2.1.

	Limiting Magnitude	*Central Wavelength*	*FWHM*
KPNO U	27.1 (5σ)	3552 Å	630.71 Å
F435W	27.8 (10σ)	4297 Å	1100 Å
F606W	27.8 (10σ)	5907 Å	2500 Å
F775W	27.1 (10σ)	7764 Å	1700 Å
F850LP	26.6 (10σ)	8950 Å	900 Å

Table 2.1-The limiting magnitude, central wavelength and width of the Ubviz filters

Since UV radiation we observed is sensitive to dust absorption in a galaxy, UV star formation rate will be underestimated by extinction. So now we need radio radiation from a galaxy because radio radiation (long wavelength) is not affect by extinction. We will derive the radio star formation rate from the radio flux of galaxies, the radio SFR should infer intrinsic star formation rate. Because UV and radio radiation also generate

by high-mass star, so we can use the radio-to-UV SFR ratios to infer dust absorption. Because of the improvement of radio observation, we adopt VLA 1.4 GHz GOODS-N catalog from Morrison et al. (2010), which have 1230 objects with 5σ.

We adopt 2MASS K_s catalog from Wang et al. (2010), the limiting magnitude reach 24.45 under 5σ, for the $z - K_s$ analysis in Chapter 5. To exclude the X-ray source (i.e., removing AGNs), we adopt Chandra X-ray 2 Ms point-source catalog from Alexander et al. (2003), exclude the objects with X-ray detection. Matched all the catalogs, there are 80 objects left.

Figure 2.1 indicates the sample distribution.
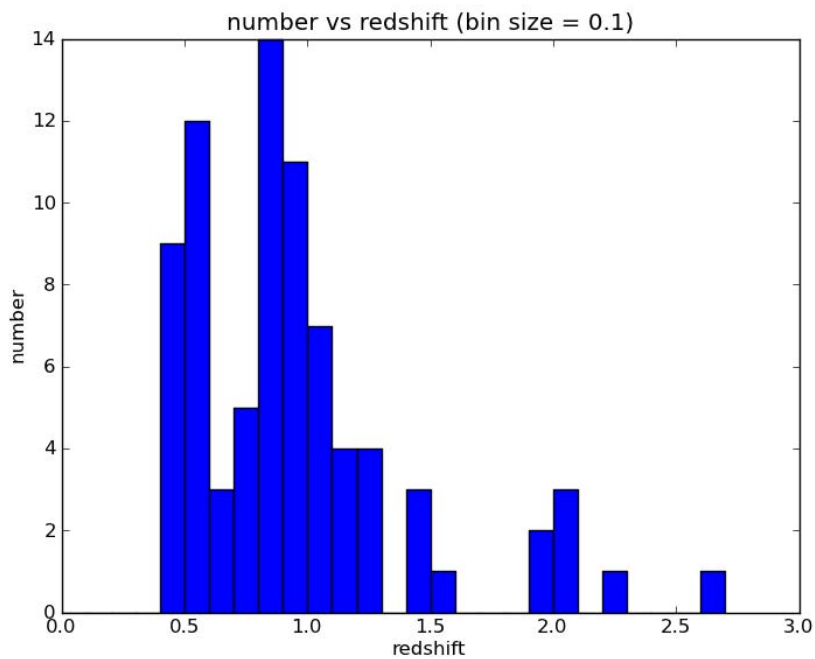
Figure 2.1-Sample distribution

Most of the objects distribute over 0.5~1.5 in redshift, the highest redshift in this samples is ~2.6. Objects with redshift less than ~0.4 is excluded because rest-frame UV (1300~3500 Å) just cover one band (or none) in the fitting of UV spectral slope, we will mention in Chapter 3.

Chapter 3   UV Spectral Slope

To study star formation rate of star forming galaxies, we have several ways to obtain SFR, UV SFR, radio SFR, inferred SFR etc.. We know well about the stars' features compare with other features in a galaxy, (i.e., we know well about how high mass star radiate UV radiation) so the UV SFR is one of the most reliable parameters of galaxy.

However, we need to concern about that dust absorption will largely affect the observation, especially in UV. It's mainly believe now that UV spectral slope (β) is correlated with extinction, large β infer large extinction. Then obtain extinction magnitude to correct for the absorbed part to obtain the intrinsic UV spectrum and SFR.

3.1   Definition of UV Spectral Slope

UV spectral slop (β) is defined as

$$f_\lambda = \lambda^\beta.$$
(3.1)

f_λ is flux density, measured in ergs per second per square centimeter per angstrom.

Because the observation data is given by apparent magnitude (m), so we need to derive the correlation between m and β.

In AB magnitude system, where

$$m = -2.5 \log f_v - 48.6.$$
(3.2)

f_v is flux density, measured in ergs per second per square centimeter per hertz. The AB magnitude system is defined such that for any band or filter being considered, the magnitude zero-point corresponds to a flux density of 3631 Jy. (1 Jy = 10^{-23} erg s^{-1} cm^{-2} Hz^{-1})

Consider there are two rest-frame UV magnitudes in an object, m_1 and m_2,

$$m_1 - m_2 = -2.5 \log \frac{f_{v_1}}{f_{v_2}}. \tag{3.3}$$

We know that the total energy independent with what space we choose (wavelength space of frequency space), so

$$f_\lambda \, d\lambda = f_v \, dv, \tag{3.4}$$

$$f_v = f_\lambda \frac{d\lambda}{dv}. \tag{3.5}$$

Consider equation (3.1) and $\lambda = \frac{c}{v}$, we can obtain

$$f_v \propto \lambda^{\beta+2}. \tag{3.6}$$

As we know that there is flat rest-frame UV spectrum in frequency space if galaxies have no extinction, it means that $\beta = -2$ is the case for no extinction.

So now we can rewrite equation (3.3):

$$m_1 - m_2 = -2.5 \log \frac{\lambda_1^{\beta+2}}{\lambda_2^{\beta+2}}, \tag{3.7}$$

$$m_1 - m_2 = -2.5(\beta + 2)(\log \lambda_1 - \log \lambda_2). \tag{3.8}$$

Now we can see that in log wavelength space, slope of magnitude (slope$_m$) is $-2.5(\beta + 2)$:

$$\text{slope}_m = \frac{m_1 - m_2}{\log \lambda_1 - \log \lambda_2} = -2.5(\beta + 2), \tag{3.9}$$

so

$$\beta = -\frac{\text{slope}_m}{2.5} - 2. \tag{3.10}$$

In this derivation, slope$_m$ is directly the slope of 2 points, but if there are more than 2 rest-frame UV magnitude in an object, we will use all the band within the range of

rest-frame UV (1300~3500 Å) to fit the slope$_m$.

3.2   Fitting the UV Spectral Slope

In section 3.1, we know that if we want to determine the intrinsic UV SFR, we need to know β first. In this section, we will introduce the band selection method for fitting the slope$_m$ to determine β.

As we mention in Chapter 2, there are HWFM for each band. In order to more stringent, we define the width of each band as full width 10% maximum. We adopt the magnitude of the bands within the range of rest-frame UV to do the fitting. Only the objects with at least two bands within the range will be selected to fit the slope$_m$.

For star forming galaxy, OB stars emits ionizing photon ionize the surrounding hydrogen. After the ionization and recombination process, high energy photons are transfer to low energy photons that the wavelength is almost no shorter than Lyman α (1216 Å). For this reason, star forming galaxy should have Lyman α (1216 Å) dropout, we adopt the magnitude of the bands within the range between Lyman α and 3500 Å to do the fitting.

For example, consider the case that the wavelength of rest-frame Lyman α is shorter than minimum wavelength of band A, rest-frame 3500 Å is longer than maximum wavelength of band B, so that magnitude of band A, band B and all the bands between band A and band B will be adopt to do the fitting. Figure 2.1 shows that all objects with redshift less than ~0.45 are disappear; it is because since object with low redshift, the

range of rest-frame UV can't cover 2 or more than 2 bands, so we can't obtain β from those objects.

After we determined what bands we should use for each object, we use the corresponding magnitudes to do the linear fitting in log wavelength space and obtain $slope_m$. Now we convert $slope_m$ to β via equation (3.10).

Figure 3.1 shows how β distribute over redshift. β is largely scatter at redshift lest than 1.5, and become narrow after redshift larger than 1.5. It's a reasonable result because the high redshift samples are come from Reddy et al. (2006), they use Lyman break selection method that sensitive to star burst galaxy.
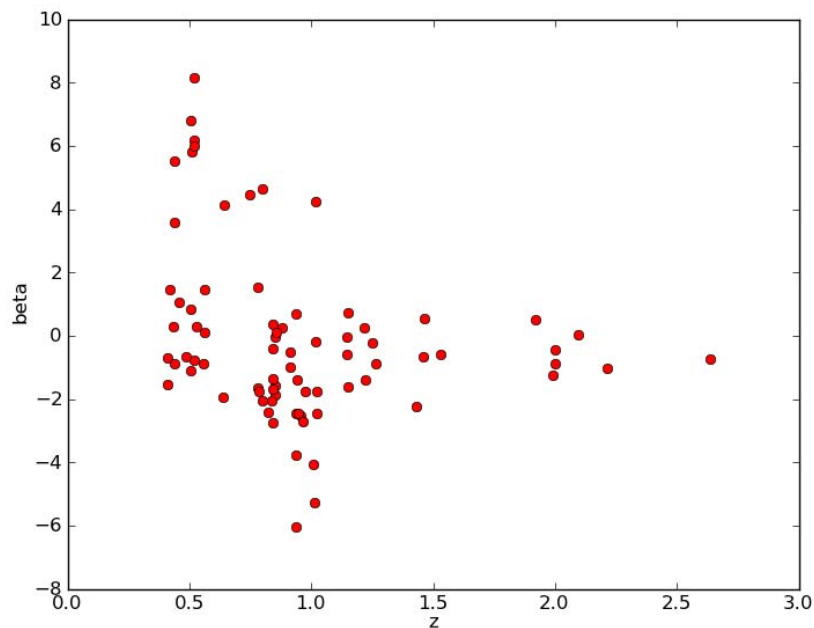

Figure 3.1-β vs. redshift

In the process of linear fitting, we assume the error of each magnitude (σ_m) is 0.05, now we see how these errors deliver to β. Consider there are N_i bands we use to do the fitting

for the i-th object, we first define Δ_i as

$$\Delta_i = N_i \sum_{N_i} \log \lambda - \left(\sum_{N_i} \log \lambda \right)^2. \tag{3.11}$$

The variation of slope$_m$ is

$$\text{Var}(\text{slope}_m)_i = \frac{N_i \sigma_m{}^2}{\Delta_i}. \tag{3.12}$$

Because of equation (3.10), the error of β (σ_β) can be write as

$$\sigma_{\beta_i} = \frac{\sigma_m}{2.5} \sqrt{\frac{N_i}{\Delta_i}}. \tag{3.13}$$

Figure 3.2 shows the distribution of σ_β, most of the object just fitted by 2 magnitudes, so they share the same σ_β about 0.42.
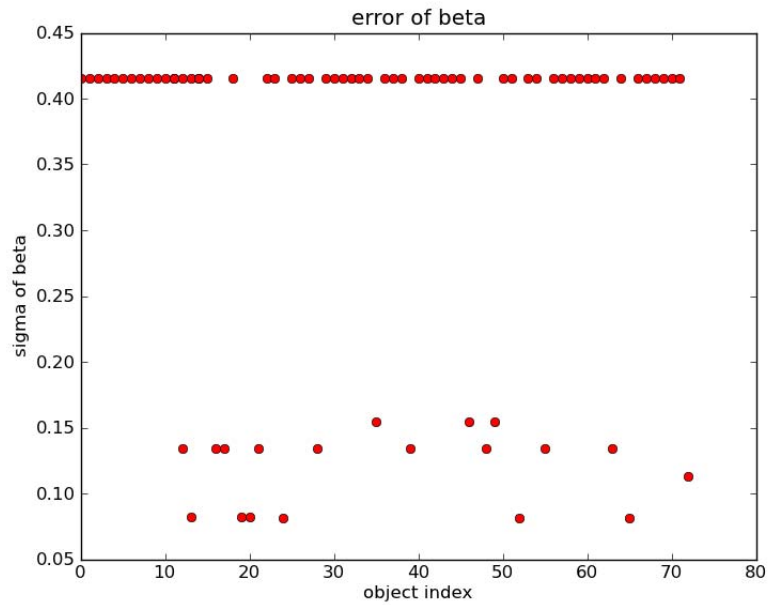

Figure 3.2-Error of β

3.3 Unusual Objects

After we defined the UV spectral slope (β), we examined the very blue objects with β < 3. There are 7 such objects, and they are shown in Figure 3.3. Some of the "blue objects"

are not really blue. We can see that object 1, 3, and 4 are all faint at U and B bands, and only bright at V and R bands, so they are not real blue objects. They are all next to other bright blue galaxies. We believe that these three objects have fluxes contaminated by nearby blue objects, and we exclude them in our subsequent analyses.
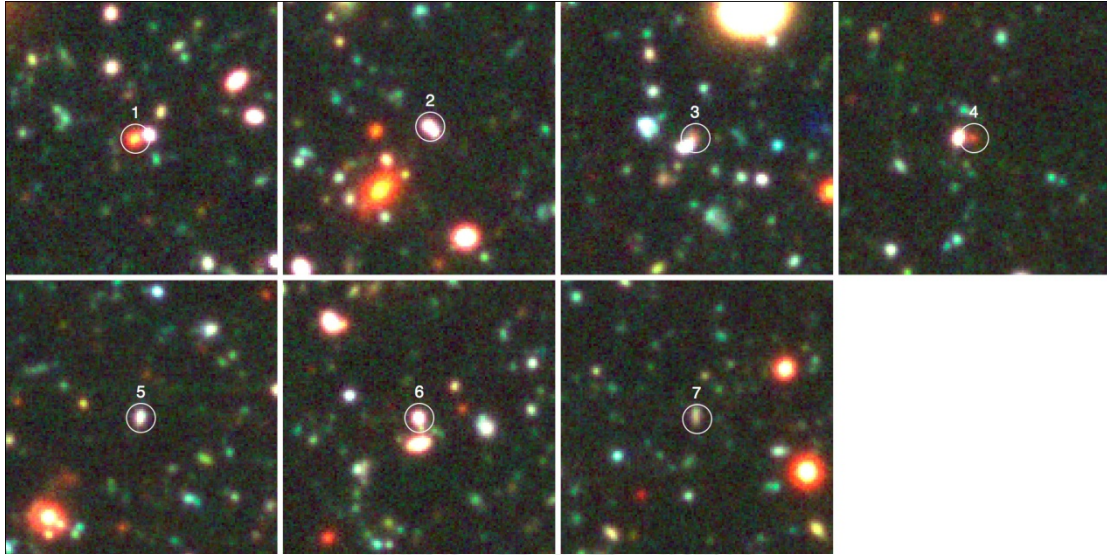
Figure 3.3-The 7 blue objects with $\beta < 3$, blue is U band, green is B band, and red is V+R band.

We also examined the 11 objects with $\beta > 2$ (very red in rest-frame UV, Figure 3.4). Objects 1, 2, 6, 7, 8 and 11 have 24 μm detections. After dust absorbs UV emission from young high mass stars, it will re-radiate the energy in the IR. So galaxies with 24 um emission are dusty star forming galaxies. Their red rest-frame UV color (large β) is likely caused by dust extinction. The objects without 24 um emission are probably non-star-forming galaxies with old stars. Their radio emission is likely from AGN but not star formation. Their red rest-frame UV color is likely caused by their old stars, but not dust. In our subsequent figures, we will use different symbol to distinguish between objects with 24 μm emissions and without 24 μm emissions for $\beta > 2$.

Figure 3.4-The 11 red objects with β > 2

After the sample selection, there are 77 objects have rest-frame UV, radio and K band flux without X-ray radiation.
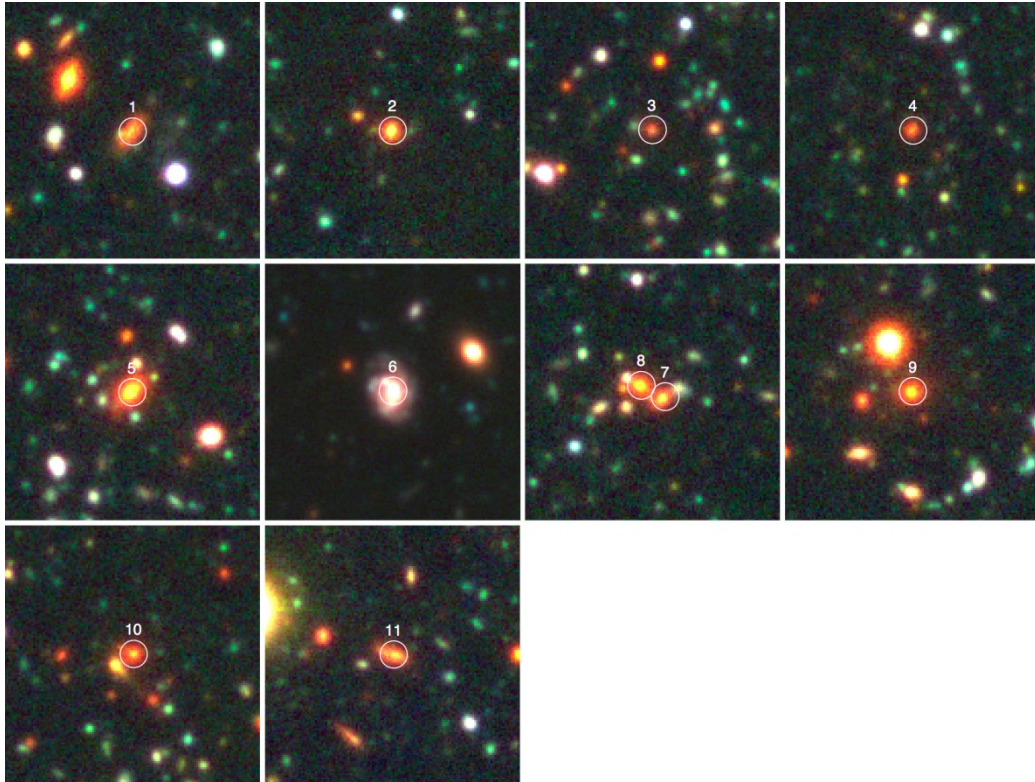
Chapter 4   Star Formation Rate

Star formation rate (SFR) is an important parameter to understand the evolution history of galaxy, the unit of SFR is solar mass per year. We can obtain star formation rate via several method, we will discuss UV star formation rate (UV SFR) and radio star formation rate (radio SFR) and how they relate to β in this chapter.

4.1   UV Star Formation Rate

There are large amount of OB stars distribute in spiral arms in star forming galaxy, we know well about how they emit strong UV radiation. So we can obtain UV SFR by observing the UV flux, then we will know how many OB stars formed per year of galaxies. Compare the OB stars forming status to initial mass function (IMF), we will understand the whole star forming history of galaxies.

We adopt the conversion between rest-frame 2800 Å UV luminosity and UV SFR in Kennicutt et al. (1998):

$$SFR(M_\odot \, yr^{-1}) = 1.4 \times 10^{-28} L_v (ergs \, s^{-1} \, Hz^{-1}). \tag{4.1}$$

This is low redshift approximation of steady state of star formation, which means SFR has remained constant over timescales that are much longer than 10^8 years.

To obtain rest-frame 2800 Å UV luminosity, we need to determine the magnitude at 2800 Å (m_{2800}). Rest-frame 2800 Å should between 2 bands, the 2 bands we use is depended on redshirt of that object, for example, band A and band B. Given the two bands, we have the magnitudes m_A and m_B, then interpolate the m_{2800} corresponding to

rest-frame 2800 Å. Table 4.1 shows the number of object which rest-frame 2800 Å fall into corresponding interval of bands in different interval of β.

	$\beta \leq -3$	$-3 < \beta < 2$	$\beta \geq 2$
UB	0	11	7
BV	4	32	4
VI	0	12	0
IZ	0	6	0
Longer than Z	0	1	0

Table 4.1-Positions of rest-frame 2800 Å of 77 objects

As we obtain the rest-frame 2800 Å magnitude (m_{2800}), equation (3.2) can lead to rest-frame f_{v2800}. To obtain rest-frame 2800 Å UV luminosity (L_v), we still need to know the luminosity distance (D_L). Ned Wright's Cosmology Calculator is a powerful tool to obtain D_L (with default parameter setting).

In the case of high redshift, the correlation between flux density and luminosity is given by

$$f_{v_{obs}} = \frac{L_{v_0}}{4\pi D_L{}^2}(1 + z). \qquad (4.2)$$

Consider a rest-frame radiation source, there is no $(1 + z)$ factor, this factor come out because the source is receding and stretching the wavelength, but the total energy remain unchanged, as result, f_v become smaller. So we need the $(1 + z)$ factor to correct to the rest-frame f_v, then the star-burst-approach equation (4.1) can be used.

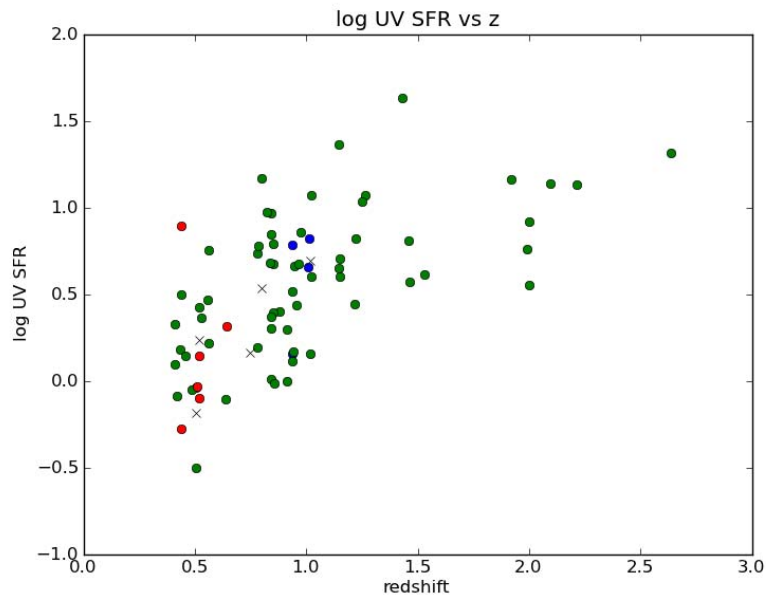Figure 4.1 shows the correlation between UV SFR and redshift.

Figure 4.1-log UV SFR vs. redshift, red points for the objects which $\beta \geq 2$, 'x' for the objects which $\beta \geq 2$ and without 24 μm detection, blue points for the objects which $\beta \leq -3$, green point for the objects which $-3 < \beta < 2$.

As expectation, there is a trend that objects with higher redshift have larger UV SFR. And there is one thing we should notice that UV radiation is sensitive to dust absorption, so we hope β can infer extinction and convert to extinction magnitude, and that's why we need to concern radio star formation rate.

4.2   Radio Star Formation Rate

For the high mass stars (i.e., OB stars), supernova explosion will be their end, under this procedure, high speed (approaching to speed of light) electrons, we call relativistic electrons, will be emitted. Once the relativistic electrons accelerated by the strong magnetic field generate by neutron stars or other objects, synchrotron radiation will be emitted, which is radio radiation. Because radio is less affect by extinction, so we can

said that radio star formation rate that calculate by radio flux able to tell us how many OB stars just explosion in a galaxy.

First we convert the radio flux ($f_{1.4GHz}$) to 1.4 GHz luminosity density ($L_{1.4GHz}$) (Wang 2012):

$$L_{1.4GHz} = 4\pi D_L{}^2 f_{1.4GHz}(1+z)^{\alpha-1},\qquad(4.3)$$

where D_L is luminosity distance, and assuming a synchrotron emission spectral slope of $\alpha = 0.8$. Since we do not have enough understanding about the intrinsic mechanism of how radio generate in entire galaxy, we can't directly convert the radio flux to radio SFR. But there is a radio-far inferred (FIR) correlation (Condon 1992), the $L_{1.4GHz}$ can be converted to $L_{FIR\,(40\text{-}120)}$ which is total luminosity between 40μm and 120μm:

$$q = \log\frac{L_{FIR(40-120)}}{3.75\times10^{12}W} - \log\frac{L_{1.4GHz}}{W\,Hz^{-1}},\qquad(4.4)$$

with $q = 2.34 \pm 0.01$ for the local case (z < 0.15) (Yun et al. 2001). We assume that the value of q will not have a large change in high redshift, so we adopt $q = 2.34$ in this work.

We also know that the total inferred (IR) luminosity between 8μm and 1000μm $L_{IR\,(8\text{-}1000)}$ is approximately 2 times of the $L_{FIR\,(40\text{-}120)}$. SFR can be converted from $L_{IR\,(8\text{-}1000)}$ (Kennicutt 1998):

$$\frac{SFR}{(M_\odot\,yr^{-1})} = 4.5\times10^{-44}\frac{L_{FIR(8-1000)}}{erg\,s^{-1}}.\qquad(4.5)$$

Combing the equation (4.3), (4.4) and (4.5), we derived

$$\frac{SFR}{(M_\odot\,yr^{-1})} = 7.83\times10^{-8}(1+z)^{\alpha-1}(\frac{D_L}{Mpc})^2\frac{F_{1.4GHz}}{\mu Jy},\qquad(4.6)$$

which is the radio star formation rate we use.

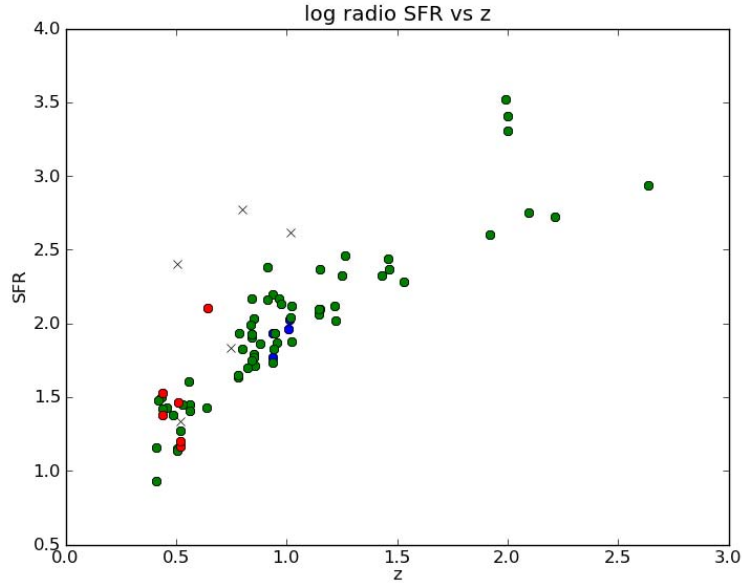Figure 4.2 shows the correlation between radio SFR and redshift.

Figure 4.2-log radio SFR vs. redshift, red points for the objects which $\beta \geq 2$, 'x' for the objects which $\beta \geq 2$ and without 24 μm detection, blue points for the objects which $\beta \leq$ -3, green point for the objects which $-3 < \beta < 2$.

We can see the detection limit here, there is no object under the imaginary parabolic curve. Interesting one is the samples with large beta tend to have large radio SFR compare with galaxies with normal β in the same redshift. But the high radio SFR objects also without 24 μm detection, these objects with strong radio flux maybe cause by active galactic nucleus (AGN), the AGN can sits in the center elliptical galaxy and have strong radio emission but no X-ray, so the X-ray catalog cannot exclude these objects then contaminate the samples.

4.3   Correlation between SFR and β

So far we know UV SFR is affected by extinction. However, if we only have UV data, we do not know whether a faint galaxy has great amount of dust or its intrinsic UV radiation is weak. Since β is come from rest-frame UV slope, large slope (red in UV) for large β, small or negative slope (blue in UV) for small β. by the definition of β, we expect that there is large β for low UV SFR, small β for high UV SFR. Figure 4.3 shows the correlation between β and UV SFR, We can see the weak trend from left-up to right-down as we expect. If β infer extinction, less extinction might lead to large observed UV SFR. However, galaxies have different intrinsic UV SFRs, so the trend here is not strong.
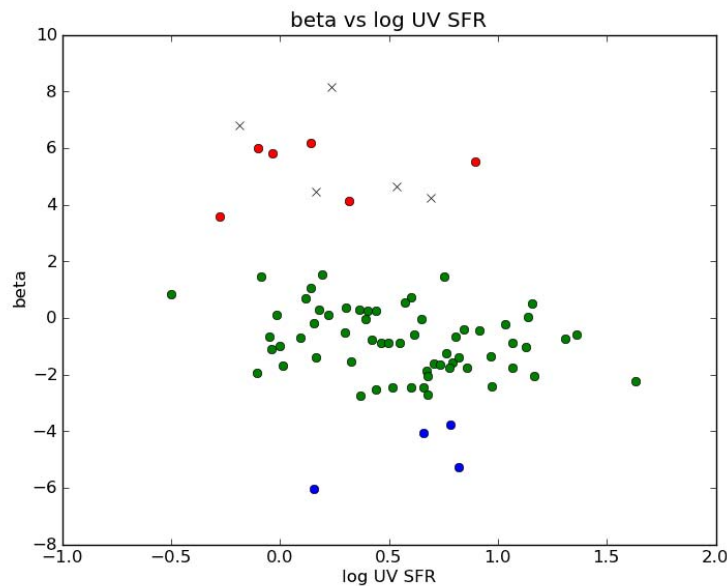

Figure 4.3-β vs. log UV SFR, red points for the objects which β ≥ 2, 'x' for the objects which β ≥ 2 and without 24 μm detection, blue points for the objects which β ≤ -3, green point for the objects which -3 < β < 2.

For the radio emission, there is no direct correlation with β. Figure 4.4 shows there are no correlation between β and radio SFR, For a given β, there is large scatter in the radio SFR.
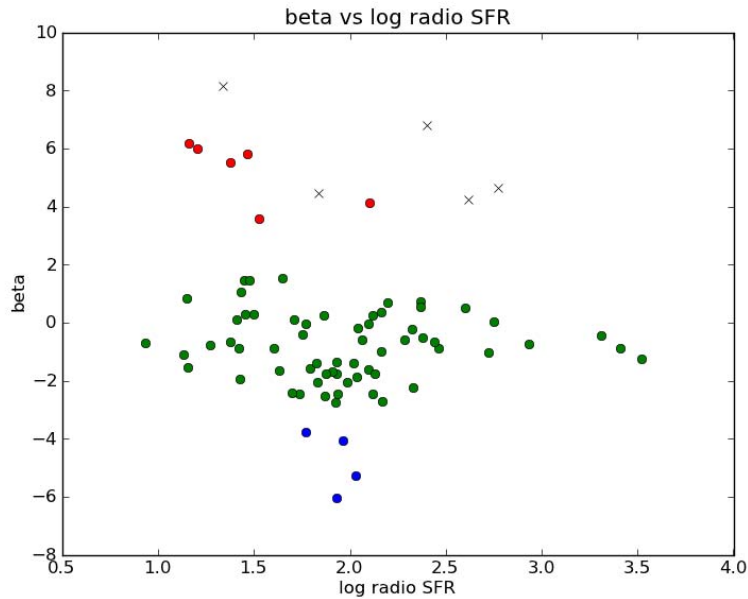

Figure 4.4-β vs. log radio SFR, red points for the objects which β ≥ 2, 'x' for the objects which β ≥ 2 and without 24 μm detection, blue points for the objects which β ≤ -3, green point for the objects which -3 < β < 2.

Astronomers mainly believe that β can infer extinction. To test this, now we introduce a parameter to indicate extinction, which is radio-to-UV SFR ratio. In a dusty galaxy, radio emission can penetrate through the entire galaxy but UV radiation would be absorbed by dust. Therefore, radio SFR represents the intrinsic star formation rate but UV SFR will be underestimated, and the correlation between radio SFR and UV SFR (radio-to-UV SFR ratio) may reflect extinction.

Figure 4.5 shows the correlation between radio SFR and UV SFR. Because both radio SFR and UV SFR infer star formation rates based on stars, if there is no dust in galaxy, the radio SFR should be equal to the UV SFR, and slope of the trend equal to 1. We can see in Figure 4.5 that for every object, radio SFR is larger than UV SFR, This implies that extinction exist in every galaxy.
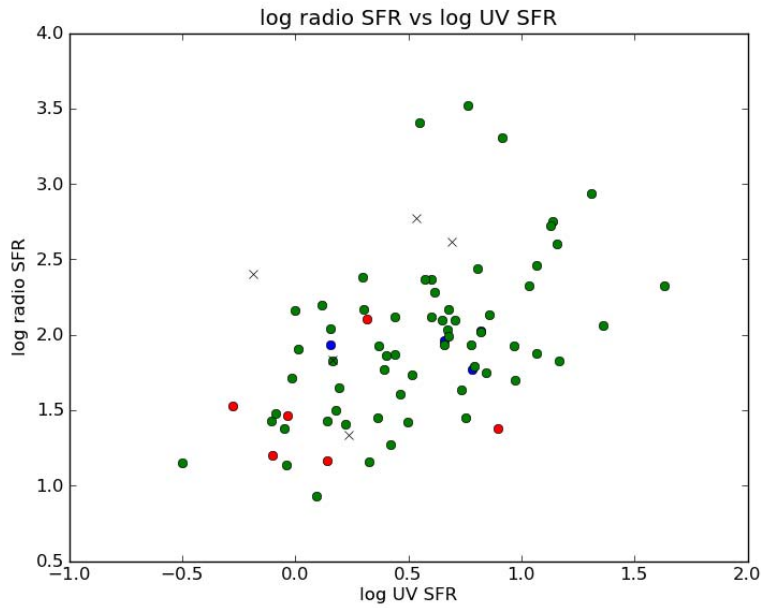

Figure 4.5-log radio SFR vs. log UV SFR, red points for the objects which $\beta \geq 2$, 'x' for the objects which $\beta \geq 2$ and without 24 μm detection, blue points for the objects which $\beta \leq -3$, green point for the objects which $-3 < \beta < 2$.

Figure 4.6 and Figure 4.7 show the correction between radio-to-UV SFR ratio and radio SFR and the correction between radio-to-UV SFR ratio and UV SFR. There is a clear trend in Figure 4.6. If we consider the SFR ratio as extinction, the dustier the galaxy is, the stronger radio emission we would observe. Figure 4.6 shows that galaxies with large intrinsic SFRs also tend to have large extinction. On the other hand, Figure 4.7 shows that galaxies with large observed UV SFRs tend to be less dusty. The two figures show

an overall consistent picture: UV radiation from galaxies is strongly affected by dust, and only radio emission can be used to reliably estimate the SFR, especially on the most active star forming galaxies.
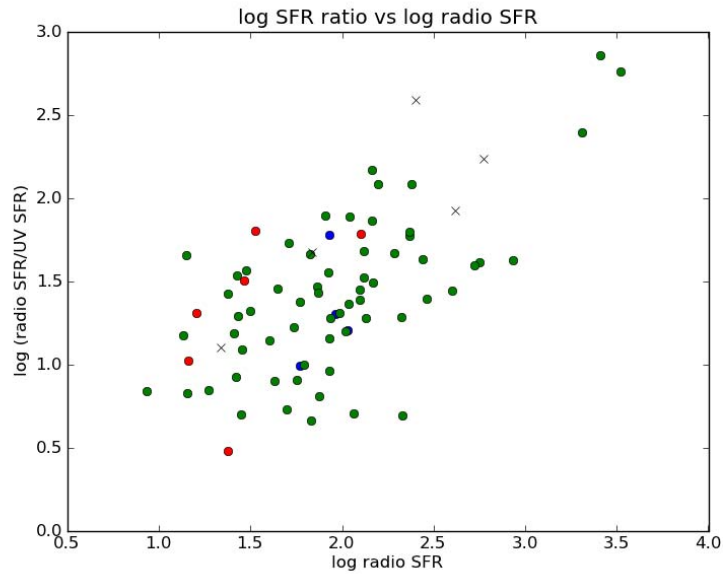

Figure 4.6-log SFR ratio vs. log radio SFR, red points for the objects which β ≥ 2, 'x' for the objects which β ≥ 2 and without 24 μm detection, blue points for the objects which β ≤ -3, green point for the objects which -3 < β < 2.
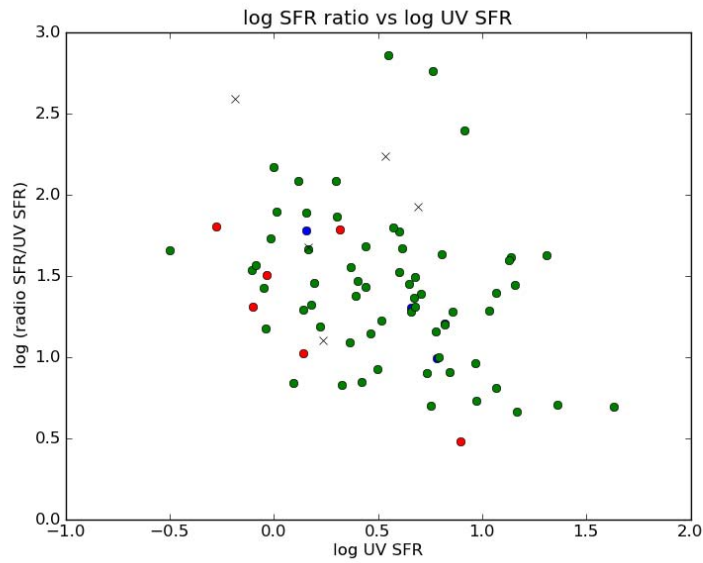
Figure 4.7-log SFR ratio vs. log UV SFR, red points for the objects which β ≥ 2, 'x' for the objects which β ≥ 2 and without 24 μm detection, blue points for the objects which β ≤ -3, green point for the objects which -3 < β < 2.

If extinction does correlate to β, there should be a correlation between radio-to-UV SFR ratio and β. Figure 4.8 shows there is not a correlation between β and SFR ratio, for a given β, there is large scatter over SFR ratio. In other words, β is not a good indicator for extinction. In next chapter, we will construct other parameters to determine if they have any correlations with the radio-to-UV SFR ratio (extinction).
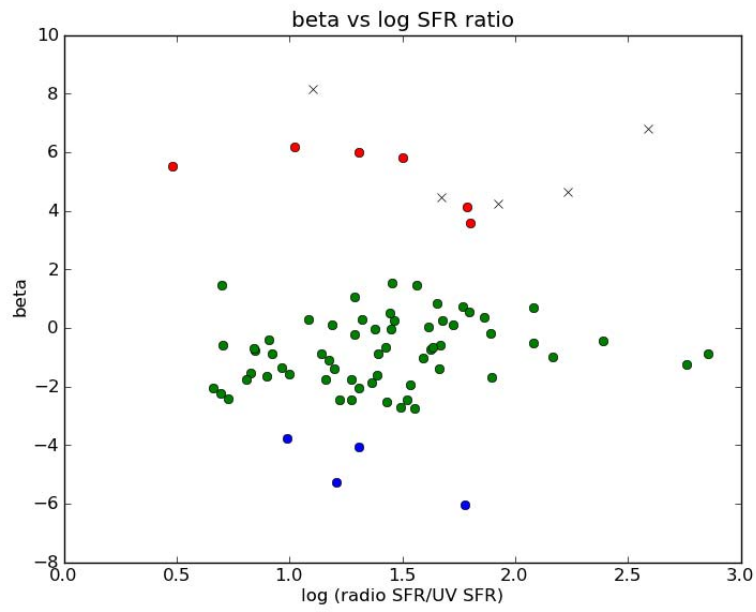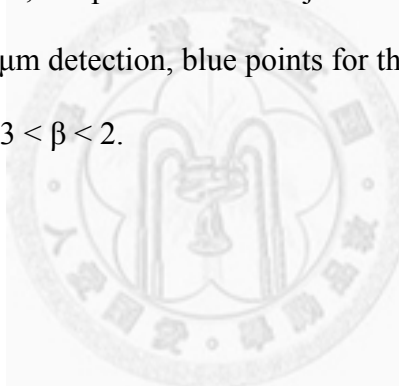
Figure 4.8-β vs. log SFR ratio, red points for the objects which β ≥ 2, 'x' for the objects which β ≥ 2 and without 24 μm detection, blue points for the objects which β ≤ -3, green point for the objects which -3 < β < 2.

Chapter 5   z – K$_s$ Analysis

As we test in 3.3, β is not a good parameter to describe extinction. Now we introduce a new parameter to find if there is any correlation with extinction, which is z – K$_s$, the F850LP magnitude minus K band magnitude. In this chapter we will examine the correlation between this long wavelength color (z – K$_s$) and the short wavelength color (β) first, then according to the feature in the z – K$_s$ vs. β diagram, we try to define new parameters to test the correlation with extinction.

5.1   z – K$_s$ vs. β Diagram

In this section, we will show the correlation between z – K$_s$ and β. The samples are the 2626 objects with redshift from catalog of Barger et al. (2008). Figure 5.1 shows the z – K$_s$ vs. β diagram. We can see in Figure 5.1 that there is a concentration region between β of -5 and 0. The distribution of the data indicates the direction of reddening: large z – K$_s$ and large β mean the galaxies are red in both long and short wavelength colors; small z – K$_s$ and small β mean the galaxies are blue in both long and short wavelength colors. However, the reddening effect could be degenerated with three other effects: the evolution of stellar population, redshift, and extinction. In the next section we use models and make assumptions to distinguish the three main effects that cause reddening in both long and short wavelength color.
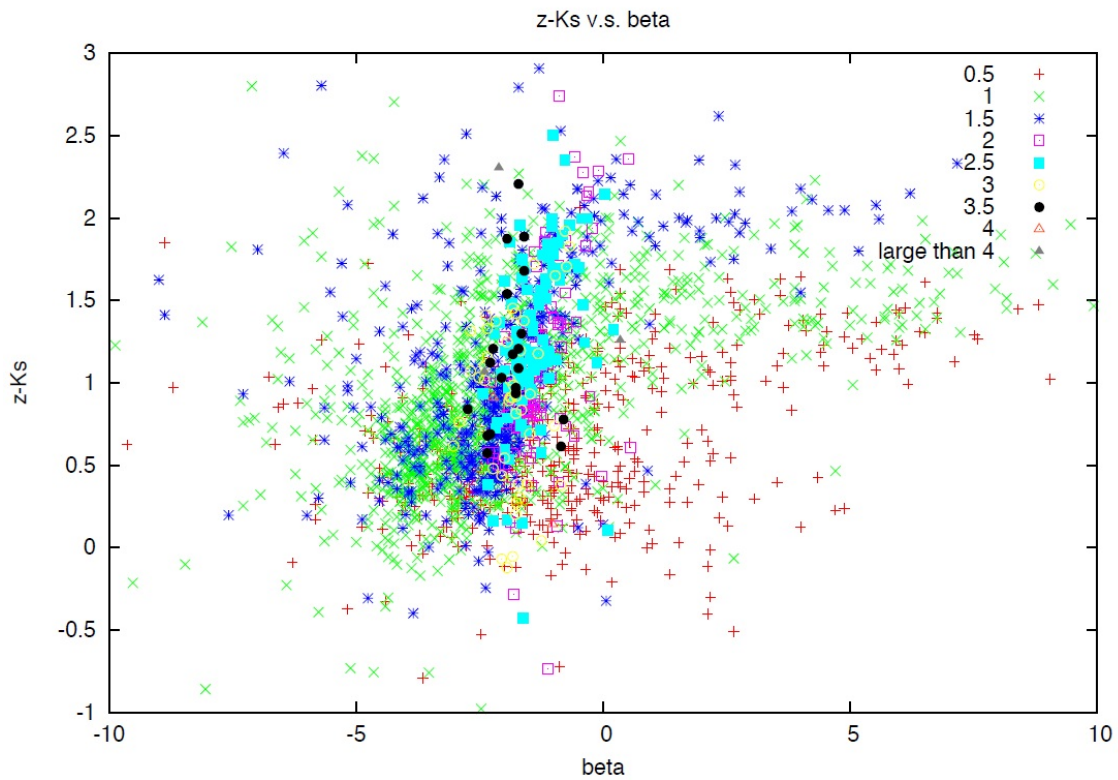
Figure 5.1-$z - K_s$ vs. β diagram, different kind of points indicate different kind of redshift as labels at right-up of the diagram. For the labels, 0.5 means redshift from 0 to 0.5, 1 means redshift from 0.5 to 1, etc...

5.2   Model and Assumptions

There are three main effects that cause reddening in both long and short wavelength color, they are stellar population, redshift and extinction. In this section we are trying to construct models to distinguish these three effects. Figure 5.2 shows the model data of different type of galaxy, the V-band extinction (A_v) and β are both derived based on the models.
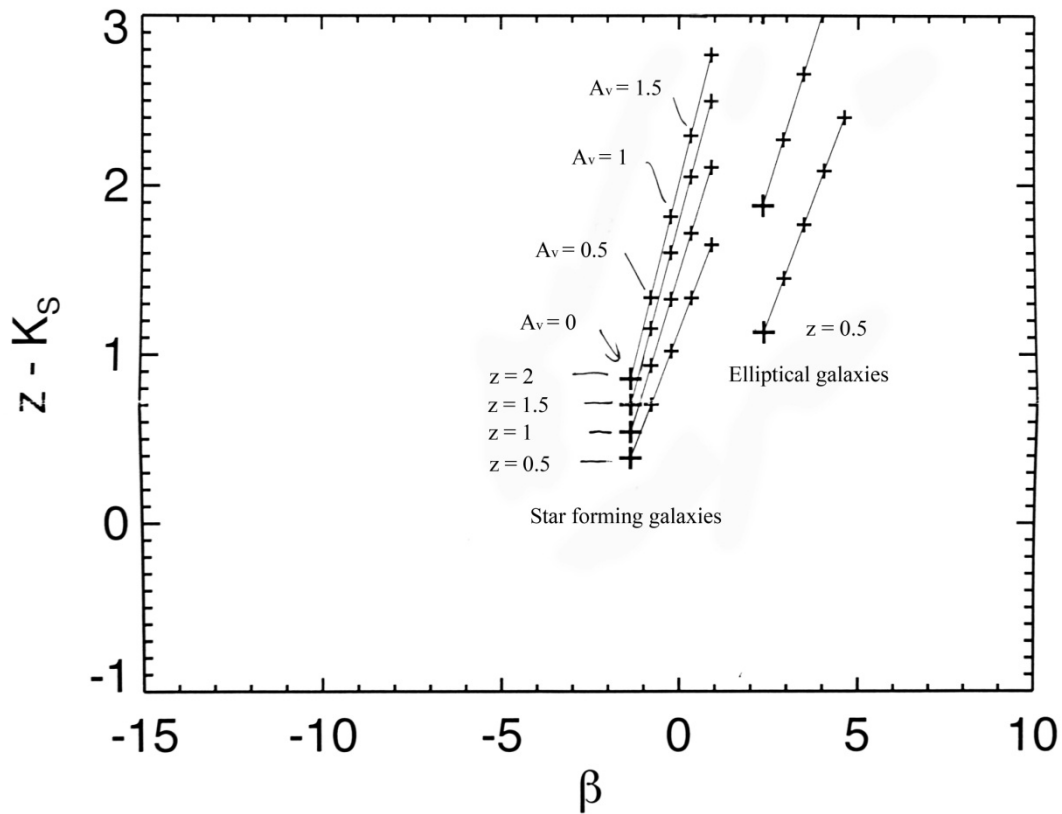
Figure 5.2-Model of the correlation between $z - K_s$ and β

We can see in Figure 5.2 that if we put a galaxy at a different redshift, β will not change. This is because β is a rest-frame property. For a galaxy at a given redshift, different extinction (different A_v) would offset its position. The offset of the trend is affected by redshift, but the movement of offset caused by redshift is less than the movement cause by extinction in the model. The offset of the trend of elliptical galaxy is quite different from that of star forming galaxy. They have large β with even zero dust absorption. If a galaxy does not occupy the region of star forming galaxies, we may classify it as an elliptical galaxy.

We notice that the direction of extinction do not follow the direction of β, and is also affect by stellar population and redshift. We will define new parameter in the next section to try to describe extinction.

24

5.3   New Parameters Test

After we show that β is not a good parameter for extinction, we try to construct other parameters to do the job, such as S and β_a. S is the distance of the data point that parallel to the elongation of the concentration region in Figure 5.1 with a arbitrary offset (Figure 5.4); β_a is the horizontal distance from the concentration region (Figure 5.6). Figure 5.3 shows the reference line for both S and β_a. The samples in here are the same as the 2626 samples in Figure 5.1. Here we separate the samples into three parts to calculate the median of each part, the range of each part is: $-0.5 \leq z - K_s < 0.5$, $0.5 \leq z - K_s < 1.5$ and $1.5 \leq z - K_s < 2.5$, the fitted line is

$$z - Ks = 0.71\beta + 2.25. \tag{5.1}$$

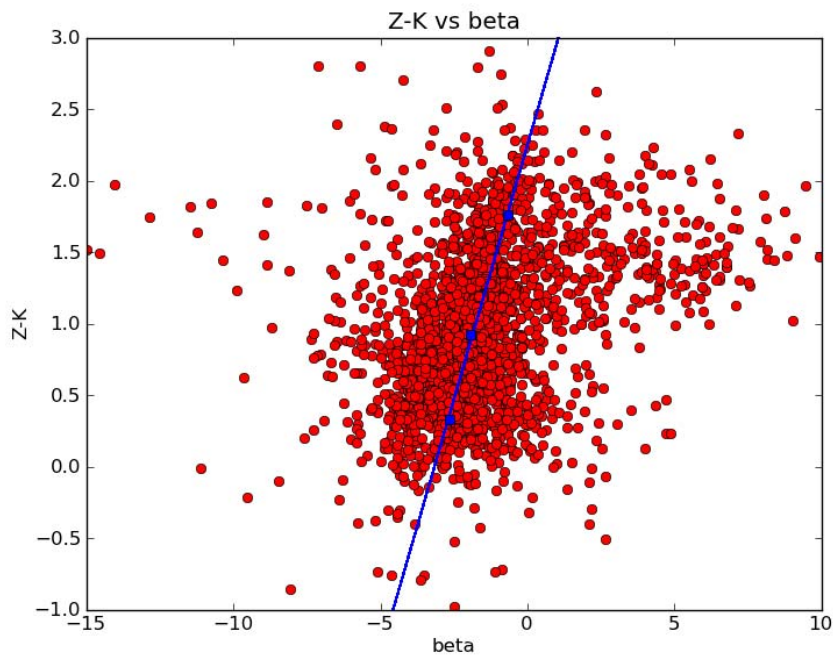This line will be used to construct the two parameters and we will introduce them in more details.

Figure 5.3-The fitting line of the trend

5.3.1 S Test

The distribution of data in Figure 5.3 along the fitted line is consistent with the expected direction of extinction based on the models in Figure 5.2. We now test that if there is any correlation with extinction. To do this, we define S to measure the distance of the sample that parallel to the line of the trend. Figure 5.4 shows how the S is defined, given a sample and an offset, we can determine S. For the offset, we need a line that is perpendicular to the line of the trend, which is

$$z - Ks = -1.41\beta + C, \tag{5.2}$$

C is set to 0 and shown in Figure 5.4 as the blue line. Each galaxy has a corresponding offset, so S for each galaxy can be determined (the red line in Figure 5.4).
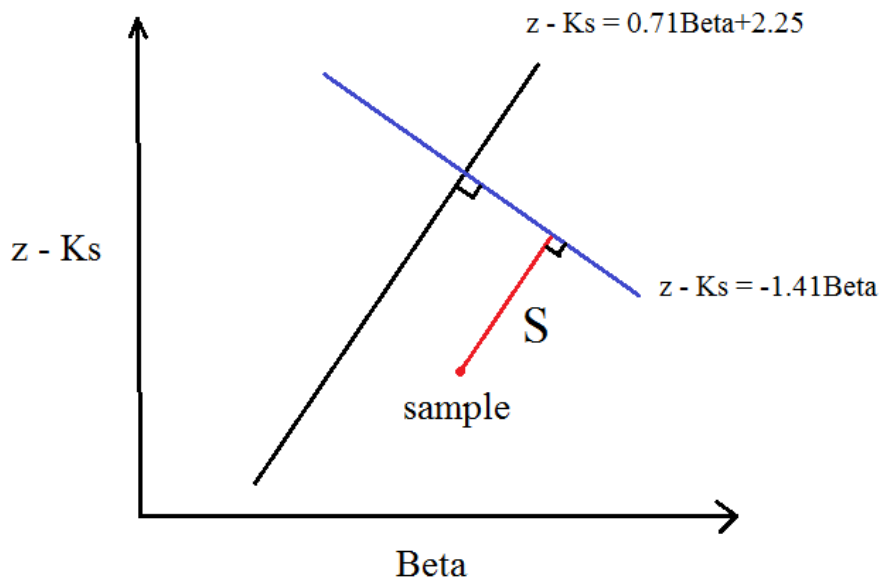

Figure 5.4-Definition of S

After we calculate all the S values for the 77 objects with radio fluxes, we plot them against the radio-to-UV SFR ratio to test the correlation (Figure 5.5). There is not a

strong correlation between S and the SFR ratio. In the model of Figure 5.2, the direction of extinction is similar to the direction of S, but not exactly the same. The stellar population and redshift could be degenerated in S.
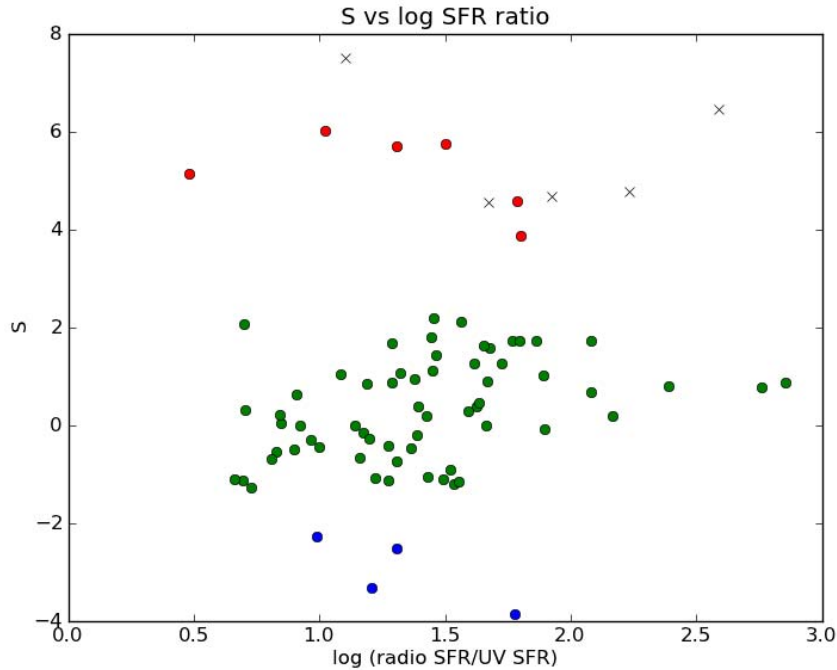

Figure 5.5-S vs. log SFR ratio, red points for the objects which $\beta \geq 2$, 'x' for the objects which $\beta \geq 2$ and without 24 μm detection, blue points for the objects which $\beta \leq -3$, green point for the objects which $-3 < \beta < 2$.

5.3.2 β_a Test

In this test, we assume that β is correlated with extinction, but different galaxy has different offset of β. Base on these assumptions, the new parameter (β_a, defined in Figure 5.6) parallel to β, and the offset of β_a change with $z - K_s$ based on the fitted line. Shown by red line in Figure 5.6, β_a could be able to obtain the correlation with radio-to-UV SFR ratio.
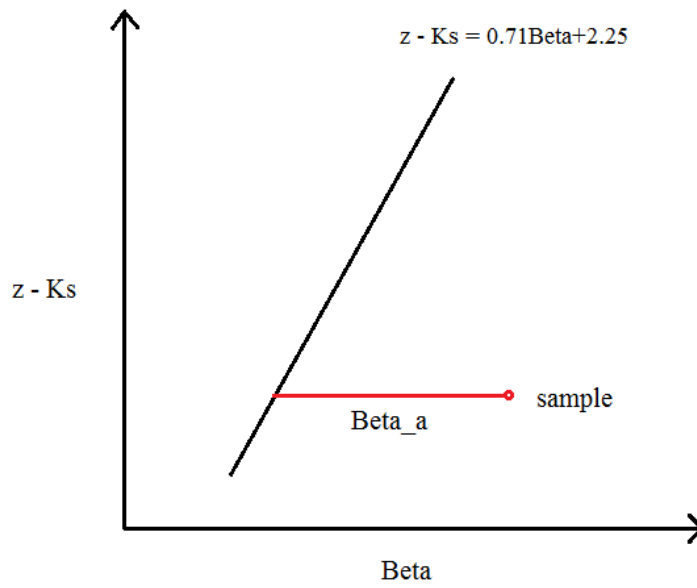
Figure 5.6-Definition of β_a

Again, Figure 5.7 shows that there is no strong correlation between β_a and SFR ratio. It could mean that evolution of stellar population do not just follow the line of the trend.
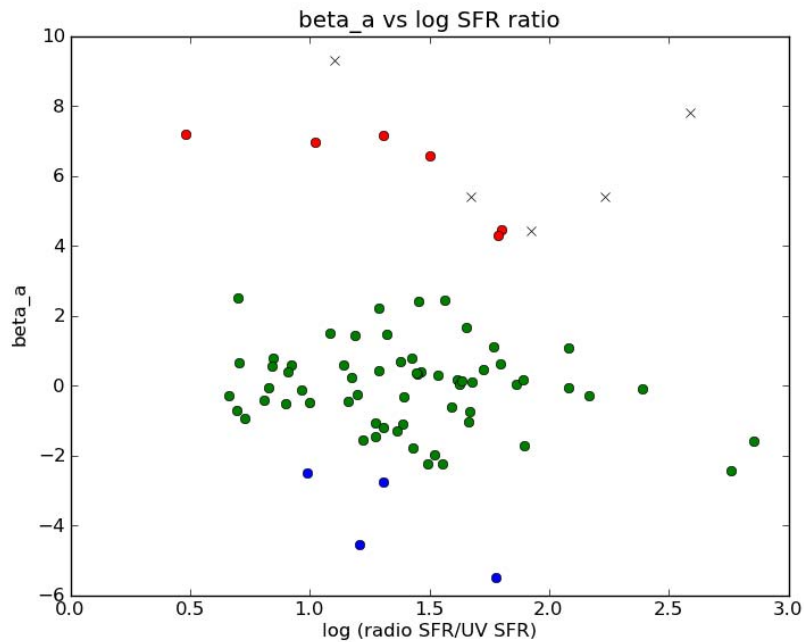

Figure 5.7-β_a vs. log SFR ratio

Chapter 6   Previous Works

There are relatively good correlation between β and extinction with starburst galaxy. In Meurer et al. (1999), they use 43 local starburst galaxies, F_{1600} is from IUE and F_{FIR} is from IRAS. The extinction indicator they use is FIR-to-UV ratio, Figure 6.1 shows that the ratio has good correlation with β, and there is a narrow range in β.
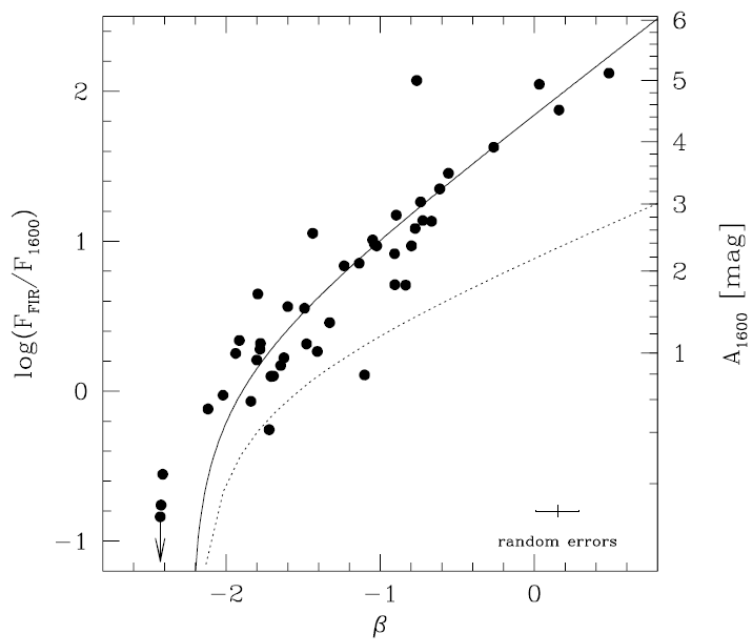

Figure 6.1- Meurer et al. (1999)

In Kong et al. (2003), they use 57 local starburst galaxies, F_{FUV} is from GALEX and F_{dust} is from IRAS. The extinction indicator they use is FIR-to-UV ratio. The correlation between the ratio and β is shown in Figure 6.2.
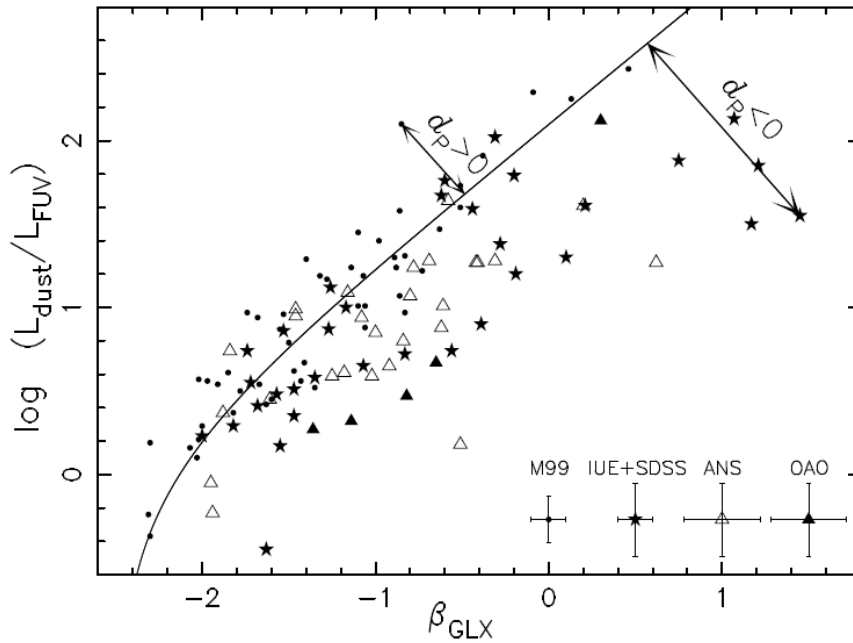
Figure 6.2- Kong et al. (2003)

Kong et al. (2003) define new parameter (d_p) to describe the scatter of sample, and they find that d_p has good correlation with 4000 Å discontinuity shown in Figure 6.3.
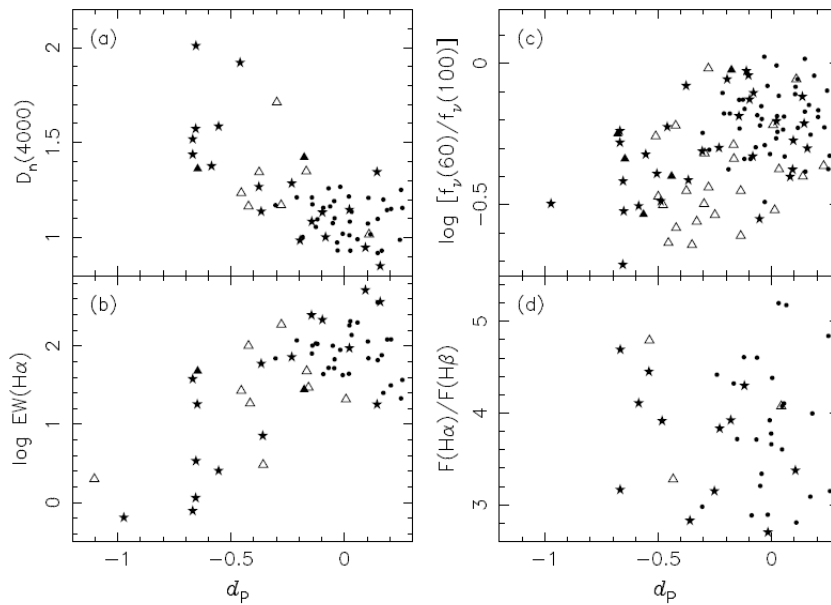
Figure 6.3-Correlation between d_p and other parameters

4000 Å discontinuity is a good indicator of star formation activity. So the scatter of sample could cause by stellar population.

In Wijesinghe et al. (2010), they use local starburst galaxies. F_{FUV} is from GALEX and F_{FIR} is from Herschel. The extinction indicator they use is FIR-to-UV ratio. Figure 6.4 shows that there is a large scatter of data.
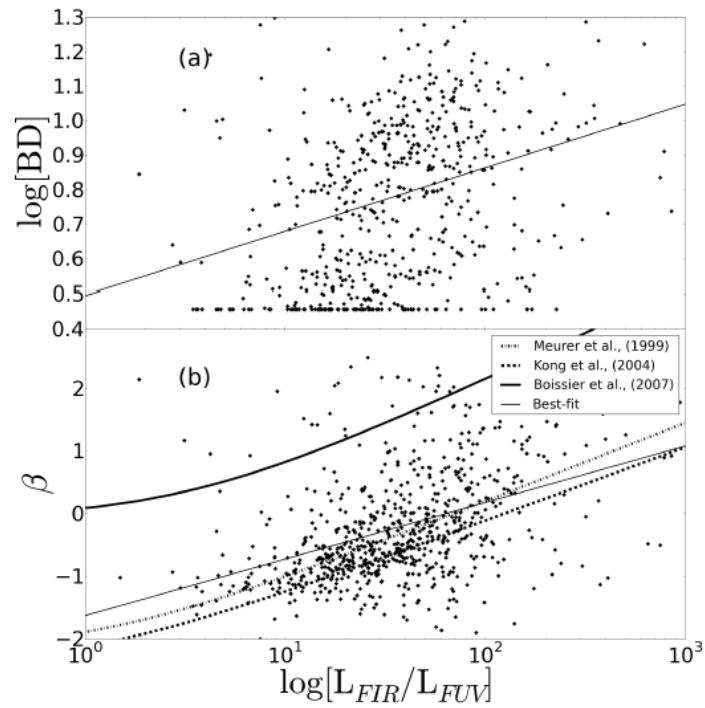

Figure 6.4- Wijesinghe et al. (2010)

Chapter 7 Conclusion

It has been widely believed that the UV spectral slope (β) is an extinction indicator, and is converted into extinction magnitude (A_v) to infer intrinsic UV luminosity. To examine if β can be used to infer extinction, we introduce radio-to-UV SFR ratio as an extinction indicator. We assume that radio is the synchrotron radiation generated by supernova explosion of high mass stars, and radio is not affected by extinction, so we can convert the radio flux to radio SFR to obtain the intrinsic star formation rate. On the other hand, since the UV emission is mainly generated by young high mass stars, and largely affected by dust absorption, the UV SFR will underestimate the intrinsic SFR. Thus, the radio-to-UV SFR ratio is a good indicator for extinction. A large SFR ratio indicates a dusty galaxy.

After we tested on correlations between β and the radio-to-UV SFR ratio, we did not find any significant correlation between them. Given a β, there is a large scatter in radio-to-UV SFR ratio, which suggests that β cannot be used as an extinction indicator. Then we defined new parameters related to β to test if there is correlation with radio-to-UV SFR ratio (extinction).

To find such new parameters, we introduced a long wavelength color, defined as $z - K_s$. Since there is a strong trend in the $z - K_s$ vs. β diagram, we defined parameter S in Figure 5.4 to describe extinction on the assumption that the direction of extinction follows the trend. The result shows that S does not have strong correlation with radio-to-UV SFR ratio, so the direction of extinction does not just follow the trend. We
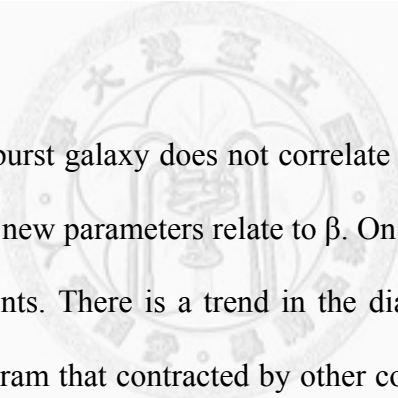
then assumed that the difference in the stellar population follows the trend, by attempting to remove the effect of stellar population from β. For this purpose, we defined β_a as a new offset for each β, and interpreted β_a as an improved extinction indicator. However we did not find a correlation between β_a and the radio-to-UV SFR ratio. Thus either S or β_a cannot be a good extinction indicator. This might caused by the contamination of AGN. We adopt the X-ray catalog to exclude the X-ray sources, but there is still a chance that AGNs sit in the elliptical galaxies and emit strong radio radiation.

The samples in other works are starburst galaxies, which are selected with rest-frame UV. There is a narrow range of β in these works, which should be caused by their UV-selection (i.e., UV-selection just picks up blue objects).
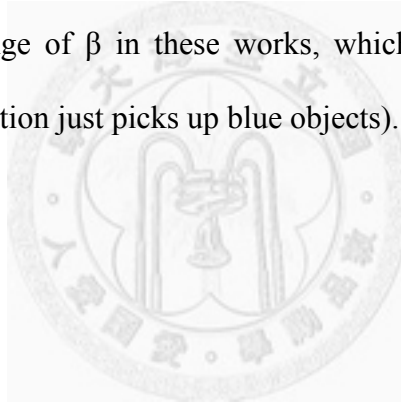
Chapter 8   Future Work

Radio emission is less affected by dust, and there is a good correlation between radio and far-inferred emission. We therefore believe that the radio-to-UV ratio is a good indicator of extinction. It is hard to observe radio for high redshift galaxy, so the number of galaxies at higher redshifts in this work is limited. We know that there is good correlation between β and extinction of starburst galaxies by other works, but it is not necessary to have good correlation between β and extinction on any galaxy. So if we do not select the data to a specific type of galaxy, we must find a new parameter to describe dust extinction.

If the extinction of non-starburst galaxy does not correlate with β, the S test and β_a test could fail because these two new parameters relate to β. On the other hand, the $z - K_s$ vs. β diagram gives us some hints. There is a trend in the diagram, and there could be a similar trend in another diagram that contracted by other color index or parameters. We need to figure out a general property in the rest-frame UV of every star-forming galaxy (not only starburst galaxy), and then we can try to construct parameters to describe extinction by different diagrams.

If we cannot find out a general property in the rest-frame UV of every star-forming galaxy, we will need to define different parameters that correlate with different types of galaxies, for example, extinction of starburst galaxy correlate with β.

REFERENCE

[1]   Alexander et al. 2003, AJ, 126, 539

[2]   Barger et al. 2008, ApJ, 689, 687

[3]   Bouwens et al. 2011, ApJ, 754, 83

[4]   Capak et al. 2004, AJ, 127, 180

[5]   Giavalisco et al. 2004, ApJ, 600, L93

[6]   Kennicutt et al. 1998, ARA&A, 36, 189

[7]   Kong et al. 2003, Mon. Not. R. Astron. Soc. 000, 1

[8]   Meurer et al. 1999, ApJ, 521, 64

[9]   Morrison et al. 2010, ApJ, 188, 178

[10]   Reddy et al. 2006, ApJ, 653, 1004

[11]   Wang et al. 2012, ApJ, 744, 155

[12]   Wijesinghe et al. 2010, Mon. Not. R. Astron. Soc. 000, 1